ISSN impresa 0717-3644
ISSN online 0718-221X

Maderas. Ciencia y tecnología 2025 (27): 41, 1-16

DOI: 10.22320/s0718221x/2025.41

LOAD-CARRYING CAPACITY OF HOUSINGS IN SOLID TIMBER BEAMS

Rafid Shams Huq[1]

Tyler Heal[1]

Thomas Tannert[1,*]

https://orcid.org/0000-0001-9699-2750

ABSTRACT

Timber framing has traditionally relied on metal fasteners, with have a high carbon footprint and often limited aesthetic appeal. These challenges can be addressed by using traditional joints such as timber housings. However, there are no design guidelines available that account for the joint geometric parameters, mechanical reinforcements, or the wood moisture content during fabrication and when loaded. In this research, the influence of joint geometry, wood moisture and reinforcement on the load-carrying capacity of solid timber beams with housings was investigated. A total of 150 *Pseudotsuga menziesii* (Douglas fir) beams were tested according standard, considering different moisture condition (wet or dry) at the time of cutting and at the time of testing. The tests confirmed that greater bearing depth and the use of self-tapping screws as reinforcement lead to increased load-carrying capacity. However, moisture condition significant affected only the double housings, not the single housings. In addition, 198 small-scale specimens were tested for shear, tension and compression to evaluate the impact of small clear specimen material strength on the beam load-carrying capacity. The results showed that these properties were weak predictors of housing performance. Finally, a design approach based on existing Canadian code provisions is suggested.

Keywords: Carpentry joints, moisture content, *Pseudotsuga menziesii,* self-tapping screws, timber framing.

INTRODUCTION

While many engineered connectors systems are gaining popularity in building construction, traditional joinery continues to offer a simple, cost effective solution (Tannert 2016). One common connection is a secondary timber beam to a primary timber beam, where the secondary member is housed into a bearing seat of the primary member for direct load transfer, as shown in Figure 1a. Such housings can be used in a single-sided configuration in beams adjacent to openings, or in double-sided configurations in floor or ridge beams. The different varieties of these joints are also called load-bearing housings, partial-width notches, butt cogs, dovetails, or beam pockets (Sobon 2014). The housing geometric parameters that will be referred to in this paper are shown in Figure 1b.

Limited testing, conducted by Nehil and Trojniak (2013), on double-sided housings in green timbers, found that capacity increased with increasing bearing depth. The failure modes depended on species, with softwoods exhibiting sudden tension perpendicular to grain failure and hardwoods exhibiting increasing load-carrying capacity developing after initial tension perpendicular splitting. As housings do not extend over the full width of the main beam, compound fracture surfaces developed. Nehil and Trojniak (2013) suggested that the housing load-carrying capacity can be estimated using the National Design Specification (American Wood Council 2018) equation for the shear strength of timber net sections below a connection with mechanical fasteners (Equation 1).

[1]University of Northern British Columbia. School of Engineering. Prince George, Canada.
*Corresponding author: thomas.tannert@unbc.ca
Received: 28.12.2024 Accepted: 20.11.2025

$$R = \frac{2}{3} F_s b d_n \qquad (1)$$

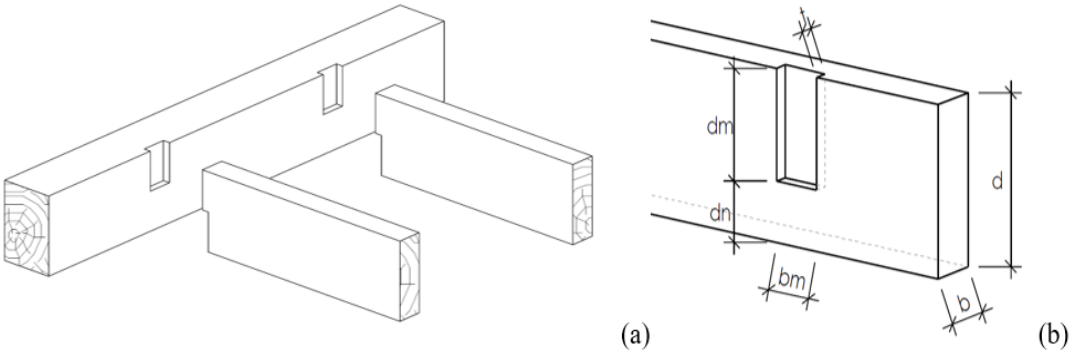

Figure 1: Typical load-bearing housing: (a) primary and secondary beams; (b) geometric parameters: d - beam depth; b - beam width; d_m - housing height; d_n - bearing depth; b_m - housing length; t - housing depth.

Where F_s is the factored shear parallel to the grain strengths, and b and d_n are the mortise geometry parameters, as illustrated in Figure 1b. However, this equation alone does not account for the bearing and splitting failure modes, which can also happen in housings.

Recent research investigated the performance of mortise and tenon joints. Xie *et al.* (2017) presented the results of an experimental study on the rotational behavior of degraded Chinese traditional mortise-tenon joints with different degradation types and different degradation degrees. Claus and Seim (2018) described the development of the multiple tenon connection, which in comparison to existing form-fitting connections, exhibit a remarkable increase of load-bearing capacity. The potential of applying the "Nuki" mortise-and-tenon joinery from perspectives of structural behavior and carbon savings was shown for modern cross-laminated timber construction (Fang and Mueller 2023). Song *et al.* (2023) investigated the fire resistance of traditional timber mortise-tenon joints and quantified the charring depth and rate, and the degradation of the rotational stiffness of the joints with fire exposure.

Wood is an anisotropic material with low strength in the perpendicular to grain direction. Hence, it is preferable to avoid or reduce stresses perpendicular to the grain. However, such stresses inevitably develop in housings. Since wood is also hygroscopic in nature, surrounding environmental conditions, i.e. relative humidity and temperature, impact its moisture content (MC), which in turn influences its mechanical properties (Sjödin and Johansson 2007). The MC of wood during construction varies based on construction material and surrounding conditions, with unseasoned green timber as often used for housings having a MC higher than 30 %. Kiln-drying (expensive) or air drying (time consuming) are used to reduce MC. However, drying leads to shrinkage of wood and strains across the cross-section. Although such stresses decrease over time due to relaxation, these stresses can lead to cracks and reduced load-carrying capacity of structural member (Dietsch 2017).

To counteract the effect of moisture-induced stresses, and to increase a connection's load-carrying capacity, several reinforcement methods exist. Self-tapping screws (STS) are the recognized state-of-the-art in fastener technology for timber structures (Dietsch and Brandner 2015, Hossain *et al.* 2018, Hossain *et al.* 2019, Hanna and Tannert 2021); they often do not require pre-drilling, are quick to install, and are therefore cost efficient. STS are produced from hardened steel and exhibit high strength and high withdrawal resistance. The thread provides a full mechanical connection along the screw's embedded length, which makes STS suited for the reinforcement of timber elements and connections prone to splitting (Tannert and Lam 2009). Jockwer *et al.* (2014) and Danzer *et al.* (2016) showed that installing STS as reinforcement is an efficient way to increase the capacities both for tension perpendicular to the grain and in shear for notched timber members. Angst and Malo (2012) studied the effectiveness of STS as reinforcement under variable climatic conditions and concluded that during wetting season in comparison to unreinforced glulam, tensile stresses were reduced.

The limited previous research on housings showed that their load-carrying capacity depends on geometric parameters. However, there are gaps regarding the understanding of how MC during fabrication and loading influence the load-carrying capacity for both unreinforced and reinforced beams. Also, the relationship between load-carrying capacity and wood strength properties has not been studied.

The objective of this study was to reduce this gap in knowledge by investigating the structural performance of timber housings, with specific focus on: i) the effect of geometric parameters on load-carrying capacity; ii) the effect of moisture changes on housings by testing dry specimens, which were fabricated under both wet (wet-dry) and dry (dry-dry) conditions and wet specimens (wet-wet); iii) the relationship between the small specimen wood strength (shear parallel to grain, tension and compression perpendicular to grain) and the housing load-carrying capacities; and iv) the influence of reinforcement with STS on housing load-carrying capacities and failure modes.

MATERIALS AND METHODS

Materials

Douglas fir (*Pseudotsuga menziesii*) beams were tested with typical sizes used in timber frame construction in Western Canada: 89 mm x 285 mm and 100 mm x 250 mm for a single-sided housing, and 184 mm x 235 mm for a double-sided housing. All timbers were graded No. 1 or better (CSA O86 2019) and were surface-planed on all four sides.

The material was received in green condition, with an average MC of 29 %, measured 25 mm below the surface using a Delmhorst RDM-2 pin-type moisture meter. The large-scale specimens were weighed just prior to testing, with an average apparent density of 601 kg/m^3 and coefficient of variation (CoV) of 10 %. The timbers were cut to length and the housings were machined with a computer numerically controlled timber processor, with the housing bases squared by hand. A paraffin wax end sealer was applied to the cut ends of all members to limit drying defects of the wet specimens. Part of the beams were air-dried by leaving them inside the UNBC Wood Innovation Research Laboratory in Prince George, Canada, for three years. The average MC of these beams after three years was 7 %.

For reinforcement, fully-threaded STS (Heco-Topix) with product approval ETA-11/0284 (DIBt 2019) with 8 mm diameter and lengths of 120 mm, 180 mm, 200 mm were selected.

Small clear specimen tests

The Canadian standard for engineering design in wood CSA-086 (2019) provides specified design values for douglas fir (*Pseudotsuga menziesii* (Mirb.) Franco), beam and stringer grades for longitudinal shear, compression perpendicular to the grain, and tension perpendicular to the grain. Herein, small clear specimen tests were conducted according to ASTM D143 (2021) to determine the actual longitudinal shear, compression perpendicular to the grain, and tension perpendicular to the grain values, as illustrated in Figure 2. Three samples for each small specimen test, with cross sections of 50 mm × 50 mm, were cut from 22 of the large-scale housing beams for a total of 198 specimens; their weights and volumes were measured to calculate the apparent density.

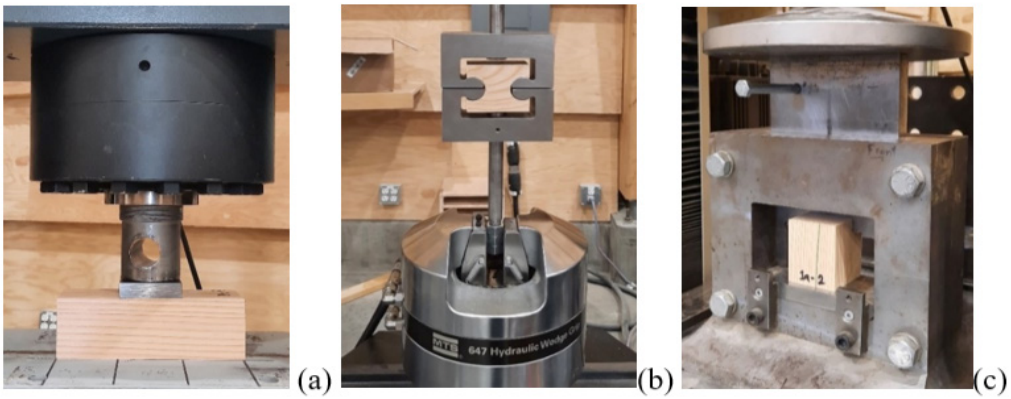

Figure 2: Small-scale specimen tests: (a) compression perpendicular to grain, (b) tension perpendicular to grain, (c) shear parallel to grain.

Housing specimen description

Four parameters were investigated: 1) Single-sided and double-sided connections; 2) Bearing depth (d_n); 3) Moisture condition during fabrication and testing; 4) Reinforcement of housing base with fully-threaded STS. The combination of these parameters led to 25 test series, as summarized in Table 1. For each series, 6 replicates were fabricated and subsequently tested, for a total of 150 specimens.

The single housing specimens had a length of 1830 mm, width of 100 mm, beam height of 250 mm, mortise depth of 25 mm, and mortise width of 89 mm. The bearing depth, the remaining depth below housing, was 57 mm for S-0.65 series and 100 mm for S-0.65 series. The double housing specimen length was also 1830 mm, width was 130 mm, and the beam height was 225 mm. Mortise width and depth were the same as in the single housings. The bearing depths were 47 mm for D-0.80 series and 82 mm for the D-0.65 series. For the reinforced housings, two STS were installed from the bottom of the beam on either side of the mortise; hence, two STS for single housings and four STS for double housings. Length of reinforcement was at least double the bearing depth. The parameters are illustrated in Figure 3 for the single housings.

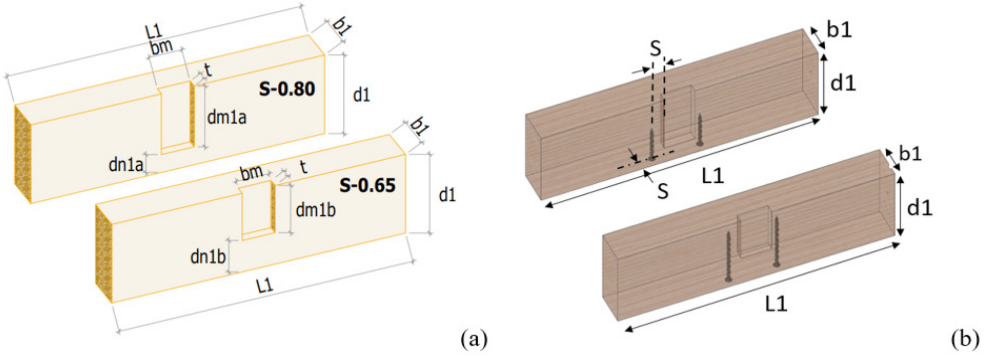

Figure 3: Schematics of single housing specimens: (a) without reinforcement; (b) with STS reinforcement.

In the series labels, the first letter refers to single (S) or double housing (D), the decimal number 0.80 or 0.65 refers to housing depth (80 % or 65 % of beam depth). The third term (WW, WD or DD) refers to the moisture conditions (wet or dry) during fabrication (first letter) and testing (second letter). WWD refers to WW specimens which were retested with reinforcement under dry conditions. The last part refers to reinforcement: none (blank), tested reinforced (R), or re-tested with reinforcement screws installed after a first test (RR). As an example, the label S-0.65-WD-RR refers to a single housing with a depth of 65 % of the beam depth, cut wet, tested dry, and then re-tested with STS reinforcement.

Table 1: Test series overview.

ID	Housing	MC	Bearing depth [mm]	Reinforcement
S-0.65-WW	Single	Cut Wet, tested Wet	100	-
S-0.65-WW-RR			100	Retested with Ø8 × 200 mm
S-0.65-WW			57	-
S-0.65-WW-RR			57	Retested with Ø8 × 120 mm
S-0.65-WW-R			57	Ø8 × 120 mm
S-0.65-WWD-RR		Cut Wet, tested Wet, retested Dry	100	Retested with Ø8 × 200 mm
S-0.65-WWD-RR			57	Retested with Ø8 × 120 mm
S-0.65-WD		Cut Wet, tested Dry	100	-
S-0.65-WD-RR			100	Retested with Ø8 × 200 mm
S-0.65-WD			57	-
S-0.65-WD-RR			57	Retested with Ø8 × 120 mm
S-0.65-DD		Cut Dry, tested Dry	100	-
S-0.65-DD-RR			100	Retested with Ø8 × 200 mm
S-0.65-DD			57	-
S-0.65-DD-RR			57	Retested with Ø8 × 120 mm
D-0.65-WW	Double	Cut Wet, tested Wet	82	-
D-0.80-WW			47	-
D-0.80-WW-RR			47	Retested with Ø8 × 120 mm
D-0.80-WW-R			47	Ø8 × 120 mm
D-0.65-DD		Cut Dry, tested Dry	82	-
D-0.65-DD-RR			82	Retested with Ø8 × 180 mm
D-0.65-DD-R			82	Ø8 × 180 mm
D-0.80-DD			47	-
D-0.80-DD-RR			47	Retested with Ø8 × 120 mm
D-0.80-DD-R			47	Ø8 × 120 mm

Test methods

The specimens were tested in a Universal Test Machine (UTM), such that the mortise was loaded in shear only, as shown in Figure 4. The secondary beam was simulated by use of loading block inside the mortise, made of Laminated Veneer Lumber, with dimensions to precisely fit into the respective mortise. Lateral restraints were provided on the outside surface to ensure that they did not deflect outwards under loading. A high-density polymer layer was inserted between the loading block and the back face of the housing to prevent any friction forces from developing. ISO 6891 (1983) was followed, loading the specimens at 5 mm/min to approx. 40 % of their expected load-carrying capacity F_{ult}, after a 30 sec hold, the load was reduced to 10 %, and after another 30 sec hold, the housing was loaded to failure, with failure defined as 80 % drop from F_{ult}. If specimens exhibited significant post-peak behaviour, tests were typically stopped at 10 mm deflection past peak load. The displacement and applied load were obtained from the UTM data acquisition system; the crack opening on either side of the housing base(s) were collected using string pots, Celesco Model SP1-25-3, attached close to the housings as shown in Figure 4c. Two sets of data were obtained from the two sensors with the results being averaged to get mean crack opening for each test specimen.

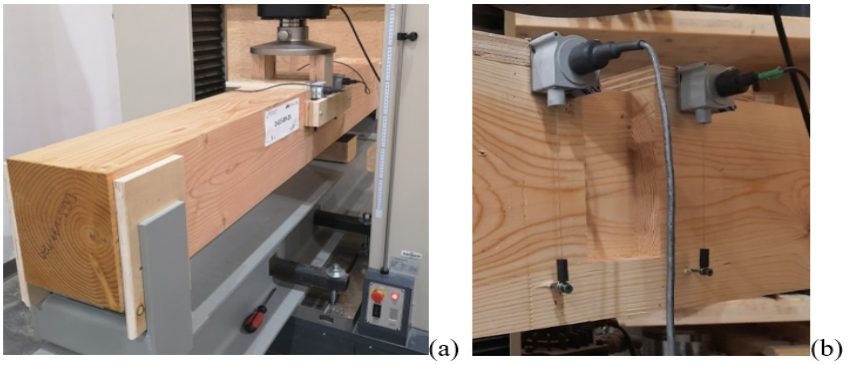

Figure 4: Experimental setup: (a) photo, (b) detail sensor.

Analyses

Analysis of variance (ANOVA) (Montgomery and Runger 2003) was conducted to determine the statistical significance of bearing depth, moisture condition, and reinforcement along with their interactions on the load-carrying capacity, F_{ult}. In order to accept or reject a null hypothesis (that there is no effect of the factor), a p-value was computed and compared to a significance level (α) of 0,05 which is typical in engineering practice (Tannert *et al.* 2012). For the single housing tests, a three-way factorial design was chosen. The first factor, bearing depth had two levels (S-0.80 and S-0.65). The second factor, MC, had three levels (WW, WD and DD) and the third factor, reinforcement, had again two levels (unreinforced and reinforced). For double housings, two-way ANOVA was performed twice. The first analysis for all DD specimens focused on bearing depths (two levels: D-0,80 and D-0,65) and reinforcement (three levels: unreinforced, retested with reinforcement, and tested reinforced) as factors. The second analysis for the D-0,80 series focused on the different moisture conditions (two levels: WW and DD) and reinforcement (three levels: -, retested with reinforcement and reinforced) as factors.

RESULTS AND DISCUSSION

Small clear specimen tests

In the compression perpendicular to the grain tests, see Figure 5a, the load at 2,5 mm compression was recorded as strength. In the tension perpendicular to grain tests, all specimens showed distinct failure at the middle of the cross-section, see Figure 5b. In the shear tests, all specimens failed by fracture through the shear plane pieces, see Figure 5c. The mean strength values for compression perpendicular to the grain, tension perpendicular to the grain, and shear parallel to the grain, their respective CoVs, as well the corresponding average densities are reported in Table 2. CSA-086 (2019) provides specified design values for Douglas Fir-Larch, beam and stringer grades for compression perpendicular to the grain (f_{cp}=7 MPa), longitudinal shear (f_v = 1,5 MPa), and tension perpendicular to the grain (f_t = 2 MPa, value from Glulam). Converting these values to mean values and adjusting them to the 7 % MC using the USDA Wood Handbook (2010) procedure results in 7,5 MPa, 2,4 MPa and 8,6 MPa for compression perpendicular to grain, tension perpendicular to grain, and shear parallel to grain, respectively. The test results are slightly higher for compression and shear and 20 % lower for tension.

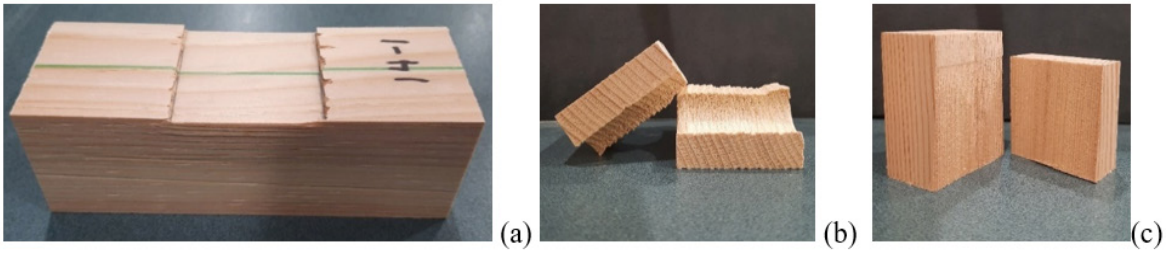

Figure 5: Failure modes of: (a) compression; (b) tension perpendicular; (c) shear parallel.

Table 2: Results from small-scale specimen tests.

Series		Compression	Tension perp.	Shear par.
S-0.80	Mean strength (MPa)	9,8	1,9	10,4
	CoV (%)	16	20	10
	Density (kg/m^3)	457	465	
S-0.65	Mean strength (MPa)	8,6	2,2	9,7
	CoV (%)	18	17	12
	Density (kg/m^3)	535	525	
D-0.80	Mean strength (MPa)	9,5	2,0	10
	CoV (%)	18	35	9
	Density (kg/m^3)	528	518	
D-0.80	Mean strength (MPa)	9,1	1,9	10,5
	CoV (%)	24	27	15
	Density (kg/m^3)	503	535	
Average	Strength (MPa)	9,3	2,0	10,2
	CoV (%)	19	25	12

Housing failure modes

Three distinct failure modes and the corresponding typical load-displacement curves, as shown in Figure 6 and Figure 7, respectively, were observed: 1) bearing, 2) splitting, and 3) hybrid mode of bearing and splitting. Bearing failure and load-displacement, shown in Figure 6a and Figure 7a, was characterized by compression perpendicular to grain of wood fibers at the housing base. These failures typically did not result in a peak ultimate load, as the wood continued to densify with increasing load. Splitting failures and load-displacement, shown in Figure 6b and Figure 7b, were caused by the perpendicular to grain tensile and/or shear parallel to grain stresses exceeding the material strength. Small cracks initiated at the housing base at a relatively low load, typically from 4-8 kN. Depending on the specimen geometry, these would then begin to propagate around 6-12 kN. Stable crack growth then continued with increasing load, until a sudden failure and drop of load carrying capacity occurred. Horizontal splits through the full width of the member were most common but varied based on the natural characteristics of each specimen, including knots, slope of grain, and pitch pockets. In the hybrid failure mode, shown in Figure 6c, splitting happened after bearing failure occurred, where the load continued to increase due to densification of the wood fibres followed by a sudden drop at load-carrying capacity. However, the splitting observed here was mostly limited to corners of the mortise base.

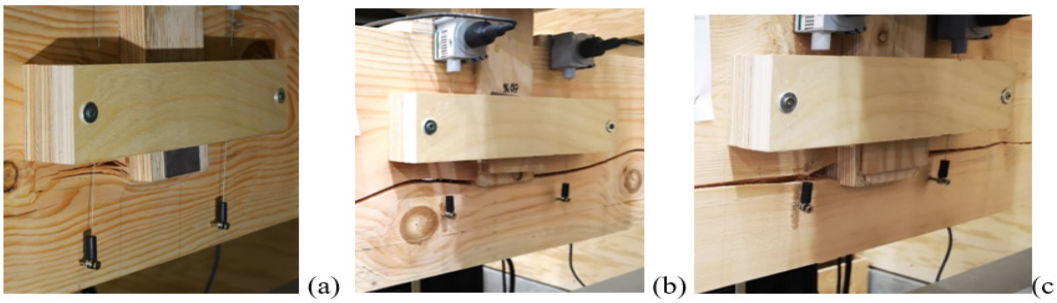

Figure 6: Typical failure modes of non-reinforced housings: (a) bearing; (b) splitting, (c) hybrid.

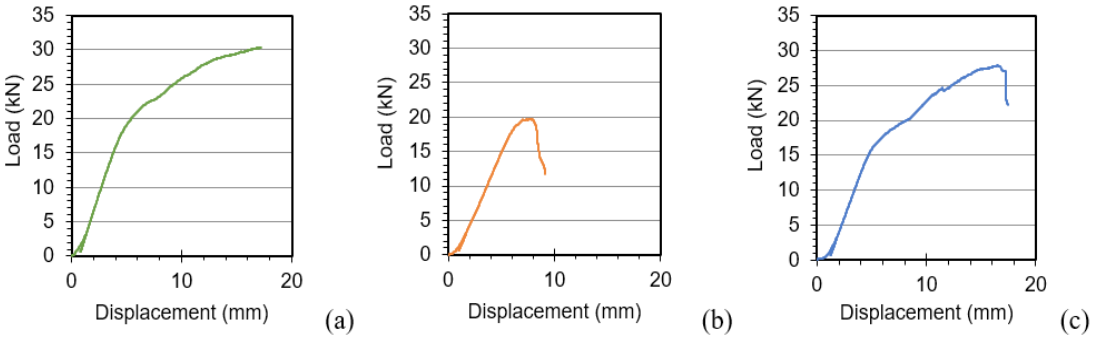

Figure 7: Typical load-displacement curves of non-reinforced housings: (a) bearing; (b) splitting, (c) hybrid.

Proportion of failure modes

The analyses of the failure modes revealed that for the unreinforced S-0.65 series, splitting accounted for 89 % of failure in S-0.65 series and 33 % in the S-0.65 series; reinforcing reduced the splitting failures to 39 % and 22 %, respectively, see Figure 8. Hence, the use of fully threaded STS in housings shifted the failure modes towards bearing or combined bearing/splitting which are primarily governed by crushing of wood fibers. Reinforced specimens which still failed in splitting, exhibited screws withdrawal failure.

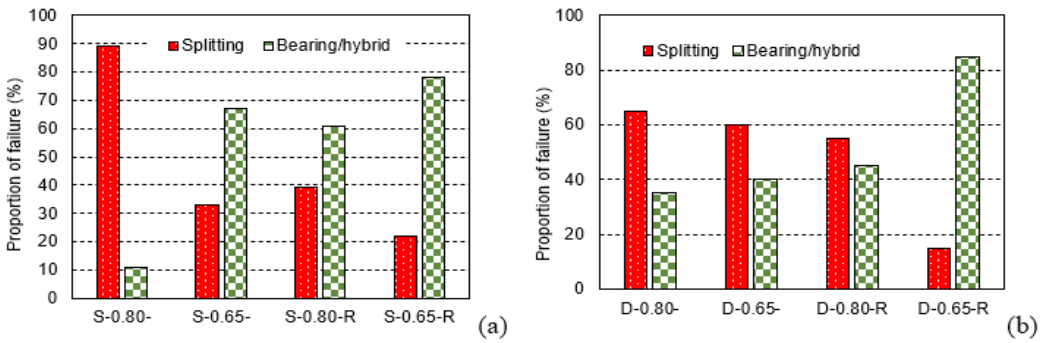

Figure 8: Proportion of failure modes: (a) single housing; (b) double housings.

In double housings, about 60 % of the D-0.80 D-0.65 and D-0.80-R series failed in splitting, while only 27 % of the specimens in the D-0.65-R series failed in splitting, see Figure 8b. Hence, in contrasts to what was observed in the single housing series where only S-0.65 series had a high proportion of splitting, the failure in double housings was significantly influenced by tension perpendicular to grain directions irrespective of the bearing depths.

Load-displacement behaviour

Representative load-displacement and load-crack-opening curves for test series with single housings are shown in Figure 9. Specimens with reinforcement reached higher loads than the unreinforced ones and failed at larger displacements. The trend is more prominent when considering the crack-opening curves in Figure 9b and Figure 9d. In the reinforced specimens, the beams reached load-carrying capacity when the cracks opened up significantly more. When comparing Figure 8a and Figure 8c, it can be seen that the load-displacement for S-0.65 series was much more variable than those of the S-0.65. However, similar to S-0.65 series, reinforcement increased the load-carrying and displacement capacities. Similar to the - specimens, the reinforced specimens also showed large variability in results.

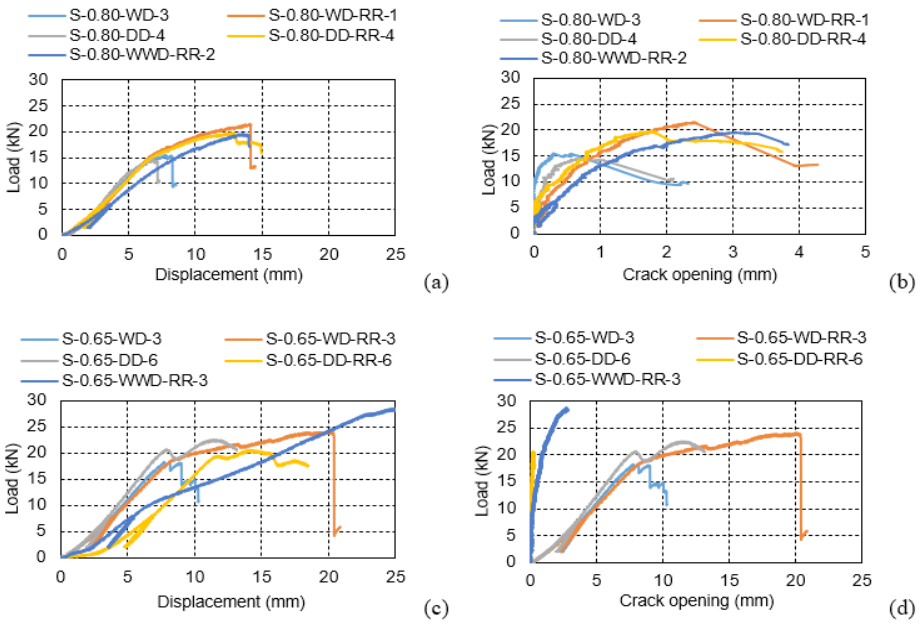

Figure 9: Typical single housing behaviour: (a) load vs displacement of 0,80 series; (b) load vs crack opening of 0,80 series; (c) load vs displacement of 0,65 series; (d) load vs crack opening of 0,65 series.

Representative load-displacement and load-crack-opening curves for test series with double housings are shown in Figure 10. The reinforced series (D-0.80-DD-R) showed higher capacity than - (D-0.80-DD) or series retested with reinforcement (D-0.80-DD-RR). The reinforcing reduced the crack opening. A similar trend can be observed with reinforced series (D-0.65-DD-R) showing higher capacity than the - (D-0.65-DD-4) and retested beam with reinforcement (D-0.65-DD-RR). Mean crack opening was small for the reinforced series (D-0.65-DD-R-1) with the retested beam reinforcement (D-0.65-DD-RR-2) showing very large crack openings before failure.

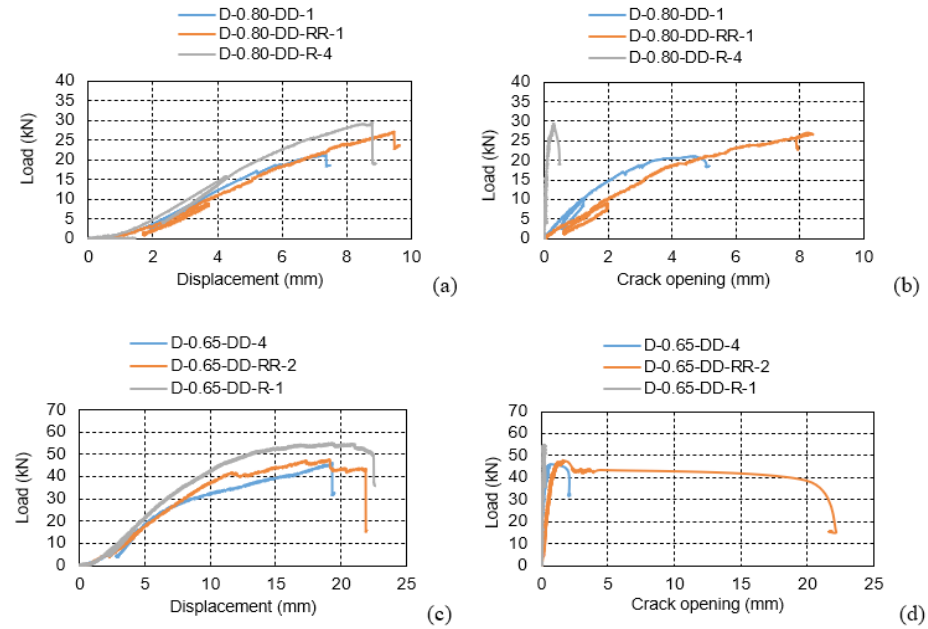

Figure 10: Typical double housing behaviour: (a) load vs displacement of 0,80 series; (b) load vs crack opening of 0,80 series; (c) load vs displacement of 0,65 series; (d) load vs crack opening of 0,65 series.

Load-carrying capacities and displacements at F_{ult}

The mean values along with their CoVs for load-carrying capacity F_{ult}, as well as mid-span displacement and crack opening at F_{ult} and densities are presented in Table 3. The mean density for single housing specimens varied from 451 kg/m^3 to 591 kg/m^3 with CoVs ranging from 8 % to 11 %. For double housing specimens, the densities ranged from 503 kg/m^3 (6 %) to 590 kg/m^3 (9 %).

For single housings, the mean F_{ult} ranged from 15 kN for S-0.65 to 27 kN for S-0.65 where lowest CoV (8 %) was obtained for S-0.65-DD and largest CoV (30 %) was for S-0.65-DD. For double housings, the mean F_{ult} ranged from 22 kN (52 %) to 50 kN (14 %) for D-0.80 and D-0.65 respectively. As in previous research (Nehil and Trojniak 2013), smaller bearing depth lead to a decrease in F_{ult}. It was not possible to directly compare single and double housings (i.e. whether the double housing capacity is twice the single housing capacity) because the depths below the mortise were not identical.

Beam displacements of single housings at F_{ult} ranged from 7 mm for S-0.65 to 24 mm for S-0.65. The lowest CoV (12 %) was obtained for S-0.65 while largest CoV (47 %) was for S-0.65. Housings with small bearing depths (S-0.65) in general exhibited larger CoVs than S-0.65; caused by the larger proportion of splitting and hybrid failure modes. For double housings, beam displacement ranged from 9 mm (20 %) for D-0.80 to 20 mm (29 %) for D-0.65.

Mean crack opening for single housings varied from 0,3 mm for S-0.65 to 2,4 mm for S-0.65. Double housings also had large variation with crack openings from 1 mm (108 %) for D-0.65 to 8 mm (81 %) for D-0.80. The CoVs were very large due to the variability in failure modes. Although crack opening is shown for all specimens, practically it only provides a meaningful metric for housings failing in splitting.

Reinforcement led to higher capacities and greater deformation before failure. The specimens which were retested after reinforcement showed higher capacities and greater deformation. Re-testing with reinforcement increased the capacity irrespective of the moisture conditions. It is interesting to note that the specimens, which were reinforced and then tested (D-0.80-DD-R and D-0.65-DD-R) had the lowest CV (9 % and 14 % respectively). Hence, reinforcing the specimens ensured lower variability.

Table 3: Test results.

ID	Density (kg/m^3)		F_{ult} (kN)		Disp. (mm)		Opening (mm)	
S-0.65-WW	475	11 %	20,1	19 %	24,5	13%	-	-
S-0.65-WW-RR			21,1	6 %			-	-
S-0.65-WW	576	9 %	15	19 %	14,9	11%	-	-
S-0.65-WW-RR			17,8	8 %			-	-
S-0.65-WW-R	591	2 %	18,3	8 %			-	-
S-0.65-WWD-RR			26,5	16 %	23,6	17 %	2,4	27 %
S-0.65-WWD-RR			17,3	26 %	10,7	23 %	2	40 %
S-0.65-WD	479	10 %	18,9	14 %	11,9	47 %	0,5	41 %
S-0.65-WD-RR			26	18 %	18,8	33 %	1,2	37 %
S-0.65-WD	455	10 %	15,4	9 %	7,2	12 %	0,3	27 %
S-0.65-WD-RR			20,6	16 %	16,6	28 %	1,9	39 %
S-0.65-DD	490	9 %	21,9	21 %	12,4	45 %	0,9	71 %
S-0.65-DD-RR			23	30 %	14,8	30 %	1	72 %
S-0.65-DD	451	8 %	14,9	8 %	7	22 %	0,8	99 %
S-0.65-DD-RR			19	17 %	10	28 %	1,5	16 %
D-0.65-WW	570	5 %	45,3	13 %	18,7	15 %	-	-
D-0.80-WW	582	9 %	31,3	20 %	10,3	12 %	-	-
D-0.80-WW-RR			39,8	14 %	16	11 %	-	-
D-0.80-WW-R	590	11 %	43,7	11 %	15,4	21 %	-	-
D-0.65-DD	506	6 %	44,3	19 %	15,6	41 %	1,2	91 %
D-0.65-DD-RR			45,6	24 %	20,0	29 %	1,9	29 %
D-0.65-DD-R	515	9 %	49,6	14 %	17,5	37 %	0,9	108 %
D-0.80-DD	510	6 %	22	52 %	8,6	20 %	3,7	86 %
D-0.80-DD-RR			26,1	28 %	13,7	41 %	8,2	81 %
D-0.80-DD-R	503	6 %	32,7	9 %	10,7	12 %	1	33 %

Detailed analyses of single housings

The impact of bearing depth on housing load-carrying capacity is illustrated in Figure 11a. The mean capacities of unreinforced S-0.65 and S-0.65 series were 17,2 kN and 22,5 kN, respectively. Hence, the 75 % larger bearing depth (100 mm vs 57 mm) resulted in a 31 % increase of F_{ult}. The higher capacity is provided by the larger ratio of bearing depth to beam depth to resist splitting. As illustrated in Figure 10b, STS reinforcement increased F_{ult} in all test series irrespective of moisture conditions and bearing depth. The average increase across all moisture conditions and bearing depths was 17 %. Both plots indicate that moisture conditions did not have a consistent effect on F_{ult}. While lower moisture is correlated with higher material strength, MC changes induce internal stresses. The impact of the latter was observed in the WD specimens which had the lowest F_{ult}. The WW specimens had higher F_{ult} than the WD specimens, suggesting that shrinkage and induced stresses are outweighing the strength increase.

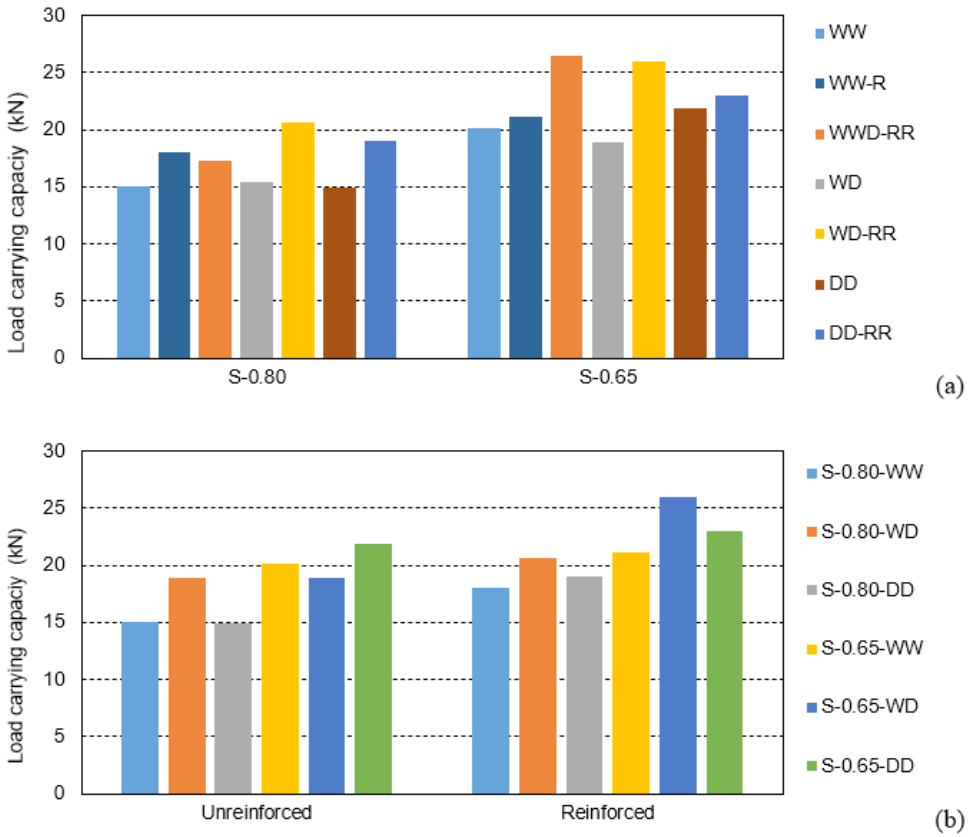

Figure 11: Single housing load-carrying capacity as function of: (a) bearing depth; (b) reinforcement.

To substantiate these findings, ANOVA was conducted. There were no significant three-way or any two-way interactions among the factors. Hence, the impact of all factors could be evaluated separately. The *p*-values for the dependent variables (bearing depth and reinforcement) were smaller than 0,05. Hence, the differences in load-carrying capacity due to variation in bearing depth and reinforcement were statistically significant. However, the influence of moisture condition was not statistically significant.

Detailed analyses of double housings

The impact of bearing depth on double housing load-carrying capacity is illustrated in Figure 12a. The mean capacities were around 27,6 kN (D-0.80 series) and 45,7 kN (D-0.65 series). Hence, the 74 % larger bearing depth (82 mm vs 47 mm) resulted in a 66 % increase of F_{ult}, substantially larger than that observed for single housings. As with single housings, the higher capacity is provided by the larger amount of material to resist splitting. As illustrated in Figure 12b, STS reinforcement increased F_{ult} in all test series irrespective of moisture condition and bearing depth. Reinforcing undamaged housings (R) was more effective with an

increase in F_{ult} of on average 29 % than reinforcing tested and cracked specimens (RR), which achieved an increase of on average 14 %. While in un-cracked beams, the load is carried by both the reinforcement and the tensile strength of wood, in cracked beams the load is carried only by the screws in withdrawal. It was further noticed that the increase in F_{ult} was substantially larger for shallow bearing depths (S-0.65) than for deeper bearing depth (D-0.80).

In contrast to single housings, the moisture conditions seemed to affect F_{ult}. However, it should be reminded that only WW and DD conditions were studied for double housings. Lower moisture should result in higher material strength; however, it also induces internal stresses. The WW specimens consistently exhibited higher load-carrying capacity, demonstrating that the influence of shrinkage and induced internal stresses are outweighing the strength increase for lower MC.

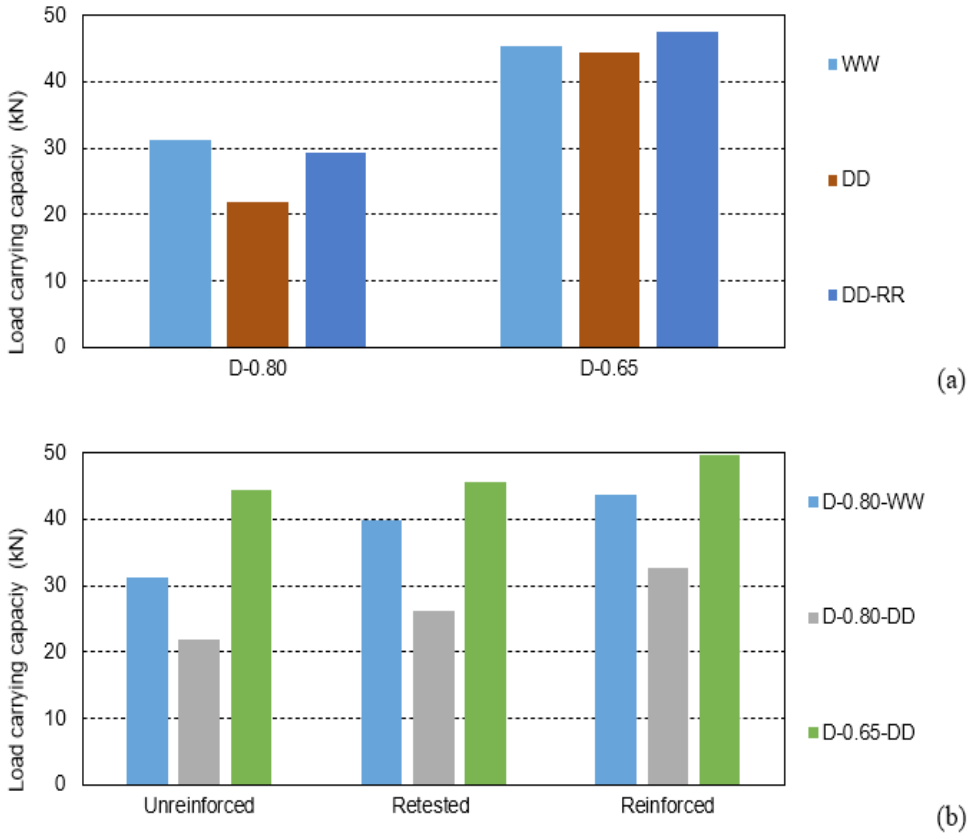

Figure 12: Double housing load-carrying capacity as function of: (a) bearing depth; (b) reinforcement.

To substantiate these findings, two ANOVAs were performed to evaluate the impact of the bearing depth, moisture condition, and reinforcement on the housing load-carrying capacity. This approach was chosen for better interpretation as the experimental design was not a complete factorial design. In Analysis 1, only the dry-dry specimens from series D-0.80 and D-0.65 were considered. The interaction between housing depth and reinforcement was not statistically significant; bearing depth was significant ($p < 0,01$), but reinforcement ($p = 0,13$) was only statistically significant if a lower confidence level of $\alpha = 85$ % was considered. In Analysis 2, all specimens from the D-0.80 series were considered. The interaction between moisture condition and reinforcement was not statistically significant; yet both the factors were statistically significant in influencing F_{ult} with $p < 0,01$; confirming that the WW series and the reinforced series exhibited larger load-carrying capacities.

Correlation between material strengths and housing load-carrying capacity

The small specimen strengths were correlated to the housing load-carrying capacity and densities, see Figure 13. The F_{ult} values were normalized for variation in mortise base depths (0,65 and 0,80) and number of housings (single or double housing). The R^2 values describe the proportion of the variation in the dependent variable (i.e., load-carrying capacity and density) which can be attributed to the independent variables (material strength). Figure 13a illustrates that compressive and shear strengths are more correlated to specimen densities with R^2 of 0,51 and 0,59, respectively, while tensile strength values only exhibit a R^2 of 0,21. While the compressive strength could be expected to be an indicator for bearing capacity of the housing, and the shear parallel and tension perpendicular strengths could be expected to be an indicator for splitting capacity of the housing. However, the very low R^2 (Figure 13b) demonstrate that the small clear specimen strengths are only a weak predictor of housing load-carrying capacity. The main reason for these weak correlations is the influence of the natural variability of solid wood, e.g. knots, grain direction, density variation, and moisture gradients.

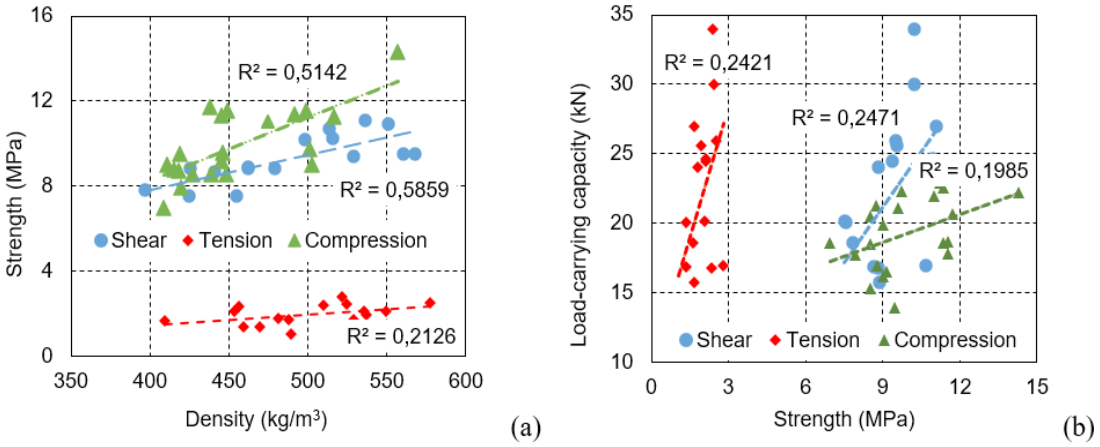

Figure 13: Material strength correlation with: (a) housing load carrying capacity, and (b) density.

Design proposal for housings

For housings reinforced with STS, it should be assumed that only the screws carry the applied load and the contribution from perpendicular-to-grain strength of the wood is ignored. The screw withdrawal resistance can be computed using either standard design provisions or those provided by the screw manufacturer. Housings with a bearing depth of less than 20 % of the beam height should be avoided, even if reinforced. For non-reinforced housings, it is suggested to adopt the CSA O86 (2019) provisions for net-shear and splitting for dowel-type connections loaded perpendicular, and for compression perpendicular to the grain bearing resistance (Equation 2).

$$R = \min\left\{ \frac{2}{3} F_s b d_n; \qquad 14(b-t)\sqrt{\frac{d_n}{1-\frac{d_n}{d}}}; \qquad F_{cp} t b_m \right\} \quad (2)$$

Where F_s and F_{cp} are the factored shear parallel to the grain and compressive perpendicular to the grain strengths, and b, d_n, t and b_m are the mortise geometry parameters, as illustrated in Figure 1b.

CONCLUSIONS

In this research, the influence of mortise geometry (single/double housings and bearing depths), wood moisture condition at fabrication and testing, and reinforcement on the load-carrying capacity of solid timber beams with housings was investigated. A total of 150 beams were prepared and tested under short-term shear loading. Based on the results, the following conclusions were drawn:

Three distinct failure modes (bearing, splitting, and hybrid) were observed. Splitting occurred suddenly, while bearing at the mortise base was not characterised by a distinct drop after reaching load-carrying capacity due to continuous crushing and densification of wood fibres at the base of the mortise. With large mortise base depths, predominantly bearing failure or hybrid failures were observed.

Confirming previous findings, smaller bearing depth (associated with mostly splitting failure) lead to a decrease in F_{ult}. The beams failing in pure splitting (beams with higher mortise depth) exhibited significantly lower F_{ult}. In single housings, a 75 % larger bearing depth resulted in a 31 % increase of F_{ult}. The impact was even more pronounced in double housings where a 74 % larger bearing depth resulted in a 66 % increase of F_{ult}.

Reinforcement with self-tapping screws increased the load-carrying capacity, shifted the failure modes towards bearing or combined bearing/splitting, and reduced crack propagation. The increase was more prominent in housings with small mortise base depths and when applied to un-cracked sections instead of reinforcing a cracked section.

For the single housing series, the moisture conditions did not consistently impact load-carrying capacity F_{ult}. For double housings, however, lower moisture contents were shown to decrease F_{ult}. While lower moisture content in timber is expected to result in higher strength properties, the moisture induced internal stresses induced and shrinkage significantly reduced the load-carrying capacity.

The low correlation between the material strengths and load-carrying capacities demonstrated that small specimen strengths are a weak predictor for the joint performance. However, adapting existing design provisions from CSA O86 (2019) does rely on using these using material strengths.

Future investigations should validate the findings by testing other species and glue-laminated timber beams. The fire resistance of housing connections, both un-reinforced and reinforced should be determined to provide guidance for the fire resistance of exposed structures with housings.

Authorship contributions

R. S. H.: Investigation, formal analysis, writing – original draft. T. H.: Conceptualization, investigation, formal analysis. T. T.: Funding acquisition; project administration, visualization, writing – review & editing

Acknowledgements

This research was supported by the British Columbia Innovation Council through funding to Dr. Tannert's BC Leadership Chair in Tall Wood and Hybrid Structures Engineering. The laboratory support provided by Michael Billups and Maik Gehloff is greatly appreciated.

Conflict of interest statement

On behalf of all authors, the corresponding author states that there is no conflict of interest.

REFERENCES

Angst, V.; Malo, K.A. 2012. Effect of self-tapping screws on moisture induced stresses in glulam. *Engineering Structures* 45: 299-306. https://doi.org/10.1016/j.engstruct.2012.06.048

American Society for Testing and Materials. 2021. Standard Test Methods for Small Clear Specimens of Timber. ASTM D143. ASTM International: West Conshohocken, USA. https://www.astm.org

American Wood Council. 2018. National Design Specification for Wood Construction. NDS. Leesburg, VA, USA. https://awc.org/publications/2024-nds/

Canadian Standards Association. 2019. Engineering Design in Wood. CSA-O86. CSA Group: Mississauga, Canada. https://www.csagroup.org/

Claus, T.; Seim, W. 2018. Development of the multiple tenon timber connection based on experimental studies and FE simulation. *Engineering Structures* 173: 331-339. https://doi.org/10.1016/j.engstruct.2018.06.102

Danzer, M.; Dietsch, P.; Winter, S. 2016. Reinforcement of round holes in glulam beams arranged eccentrically or in groups. In: Proceedings of the World Conference on Timber Engineering. Vienna, Austria.

Dietsch, P.; Brandner, R. 2015. Self-tapping screws and threaded rods as reinforcement for structural timber elements - A state-of-the-art report. *Construction and Building Materials* 101: 78-89. https://doi.org/10.1016/j.conbuildmat.2015.04.028

Dietsch, P. 2017. Effect of reinforcement on shrinkage stresses in timber members. *Construction and Building Materials* 150: 903-915. https://doi.org/10.1016/j.conbuildmat.2017.06.033

Deutsches Institut für Bautechnik. 2019. ETA 11/0284: Heco screws. European Organisation for Technical Assessment (EOTA) DIBt: Berlin, Germany. https://www.dibt.de/en/

Fang, D.; Mueller, C. 2023. Mortise-and-tenon joinery for modern timber construction: Quantifying the embodied carbon of an alternative structural connection. *Architecture, Structures and Construction* 3: 11-24. https://doi.org/10.1007/s44150-021-00018-5

Hanna, D.; Tannert, T. 2021. Glulam connections assembled with a combination of screws. *Maderas: Ciencia y Tecnología* 62(3): 1-23. http://dx.doi.org/10.4067/s0718-221x2021000100454

Hossain, A.; Popovski, M.; Tannert, T. 2018. Cross-laminated timber connections assembled with a combination of screws in withdrawal and screws in shear. *Engineering Structures* 168: 1-11. https://doi.org/10.1016/j.engstruct.2018.04.052

Hossain, A.; Popovski, M.; Tannert, T. 2019. Group Effects for Shear Connections with Self-Tapping Screws in CLT. *ASCE Journal of Structural Engineering* 145(8). e04019068. https://doi.org/10.1061/(ASCE)ST.1943-541X.0002357

International Organization for Standardization. 1983. Timber structures - Joints made with mechanical fasteners - General principles for the determination of strength and deformation characteristics. ISO 6891. ISO: Geneva, Switzerland. https://www.iso.org/home.html

Jockwer, R.; Steiger, R.; Frangi, A. 2014. Design model for inclined screws under varying load to grain angles. In: Proceedings of the International Network on Timber Engineering Research. Bath, United Kingdom.

Montgomery, D.C.; Runger, G.C. 2003. *Applied statistics and probability for engineers.* 3rd edition. Wiley: New York, USA. ISBN 978-0-471-49826-4.

Nehil, T.E.; Trojniak, B.I. 2013. Capacity of Load-Bearing Housings: Preliminary Results from Load Testing. MSc Thesis. Timber Frame Engineering Council. 195 p. https://www.tfguild.org/timber-frame-engineering

Sjödin, J.; Johansson, C. 2007. Influence of initial moisture induced stresses in multiple steel-to-timber dowel joints. *Holz Roh Werk* 65: 71-77. https://link.springer.com/article/10.1007/s00107-006-0136-6

Sobon, J.A. 2014. *Historic American Timber Joinery: A Graphic Guide.* Timber Framers Guild. ISBN (no ISBN provided). https://www.tfguild.org/store/historic-american-timber-joinery

Song, X.; Zhang, Y.; Lu, Y.; Peng, Y.; Zhou, H. 2023. Experimental study on fire resistance of traditional timber mortise-tenon joints with damages. *Fire Safety Journal* 138. e103780. https://doi.org/10.1016/j.firesaf.2023.103780

Tannert, T. 2016. Improved performance of reinforced rounded dovetail joints. *Construction and Building Materials* 118: 262-267. https://doi.org/10.1016/j.conbuildmat.2016.05.038

Tannert, T.; Lam, F. 2009. Timber Construction Self-tapping Screws as Reinforcement for Rounded Dovetail Connections. *Structural Control & Health Monitoring* 16(3): 374-384. https://doi.org/10.1002/stc.283

Tannert, T.; Vallée, T.; Hehl, S. 2012. Experimental and numerical investigations on adhesively bonded hardwood joints. *International Journal of Adhesion and Adhesives* 37: 65-69. https://doi.org/10.1016/j.ijadhadh.2012.01.014

United States Department of Agriculture. 2010. *Wood Handbook, Forest Products Laboratory.* Madison, Wisconsin, USA. https://research.fs.usda.gov/treesearch/62200

Xie, Q.; Wang, L.; Zheng, P.; Zhang, L.; Hu, W. 2017. Rotational behavior of degraded traditional mortise-tenon joints: experimental tests and hysteretic model. *International Journal of Architectural Heritage* 12(1): 125-136. https://doi.org/10.1080/15583058.2017.1390629